See discussions, stats, and author profiles for this publication at: https://www.researchgate.net/publication/325273822

Near-infrared light-guided miniaturized indirect ophthalmoscopy for nonmydriatic wide-field fundus photography

4 authors:

Devrim Toslak
University of Illinois at Chicago
28 PUBLICATIONS **47** CITATIONS

Changgeng Liu
University of Illinois at Chicago
40 PUBLICATIONS **189** CITATIONS

Minhaj Alam
University of Illinois at Chicago
12 PUBLICATIONS **12** CITATIONS

Xincheng Yao
University of Illinois at Chicago
116 PUBLICATIONS **906** CITATIONS

Some of the authors of this publication are also working on these related projects:

Functional imaging of retinal photoreceptors View project

Ultra wide field fundus photography View project

Optics Letters

Near-infrared light-guided miniaturized indirect ophthalmoscopy for nonmydriatic wide-field fundus photography

Devrim Toslak,[1,2] **Changgeng Liu,**[1] **Minhaj Nur Alam,**[1] **and Xincheng Yao**[1,3,*]

[1]Department of Bioengineering, University of Illinois at Chicago, Chicago, Illinois 60607, USA
[2]Department of Ophthalmology, Antalya Training and Research Hospital, Antalya 07030, Turkey
[3]Department of Ophthalmology and Visual Sciences, University of Illinois at Chicago, Chicago, Illinois 60612, USA
*Corresponding author: xcy@uic.edu

A portable fundus imager is essential for emerging teleme-dicine screening and point-of-care examination of eye dis-eases. However, existing portable fundus cameras have limited field of view (FOV) and frequently require pupillary dilation. We report here a miniaturized indirect ophthal-moscopy-based nonmydriatic fundus camera with a snap-shot FOV up to 67° external angle, which corresponds to a 101° eye angle. The wide-field fundus camera consists of a near-infrared light source (LS) for retinal guidance and a white LS for color retinal imaging. By incorporating digital image registration and glare elimination methods, a dual-image acquisition approach was used to achieve reflec-tion artifact-free fundus photography.   © 2018 Optical Society of America

OCIS codes: (170.0110) Imaging systems; (170.2945) Illumination design; (170.3880) Medical and biological imaging; (170.4460) Ophthalmic optics and devices; (170.4470) Ophthalmology.

Prompt screening and early diagnosis of eye diseases is essential to prevent visual impairment and blindness. Because many eye diseases can target retinal periphery, wide-field fundus photog-raphy has demonstrated its superior capability in screening, di-agnosis, and treatment evaluation of eye diseases such as diabetic retinopathy (DR) [1,2], retinopathy of prematurity (ROP) [3,4], choroidal masses, and metastases [5], and choroi-dal dystrophies [6]. Wide-field scanning laser ophthalmoscopy (SLO) systems have been demonstrated to provide wide-field fundus photography [7,8], but the high cost and operational complexity of these wide-field SLO imagers limit their clinical deployments. Traditional fundus cameras are still standard de-vices required for eye examination in both ophthalmology and optometry clinics. According to ISO 10940:2009 [9], an external-angle is commonly used to specify the field of view (FOV) in traditional fundus cameras. However, an eye angle has been recently adopted to determine the FOV in wide-field fundus imagers such as a Retcam (Natus Medical Inc.,

Pleasanton, CA), Optos (Optos Inc., Marlborough, MA). In order to avoid unnecessary confusion, we provide both ex-ternal- and eye-angle numbers in the following discussion.

It is technically challenging to construct wide-field fundus cameras. Ring-shaped transpupillary illumination has been commonly employed in traditional fundus cameras [Figs. 1(a) and 1(b)] [10]. The ring-shaped transpupillary illumination is delivered through the periphery of the pupil, and the imaging light is collected through the central area of the pupil. In order to eliminate the corneal reflection from the retinal image (RI), a buffer zone with enough distance between the illumination and observation zones [Fig. 1(b)] should be provided [11]. Otherwise, the background light due to corneal reflection will be multiple orders of magnitude stronger than the useful light back scattered/reflected from the retinal tissue and, thus, will overshadow the RI. Because only a small central pupillary area can be used for imaging purposes, and the optical system has to be sophistically optimized to guarantee that the imaged retinal area can be coincidently covered by the illumination light, the FOV of traditional fundus cameras is limited [1]. In order to achieve the necessary view field coverage, mydriatic early treat-ment diabetic retinopathy study (ETDRS) seven-field photog-raphy for DR screening has been developed based on the use of the traditional fundus camera with a 30° external angle (45° eye angle) FOV [12]. The seven-field photography requires a skilled operator for pupillary dilation and image registration to produce montage images. This hampers its clinical deploy-ments in rural and underserved areas where both expensive in-struments and skilled operators are not available.

In order to explore affordable telemedicine of eye cares, multi-ple portable or smartphone-based fundus cameras have been dem-onstrated [13–15], but existing commercially available portable fundus cameras have a limited FOV, typically a <45° external angle (68° eye angle), and frequently require pupillary dilation. By employing transpalpebral illumination, a 101° external angle (152° eye angle) FOV has been achieved in a snapshot smart-phone fundus camera [16]. However, clinical deployments of the transpalpebral illumination-based device are still challenging due to the requirement of separate adjustment and optimization of imaging and illumination sub-systems. We have previously
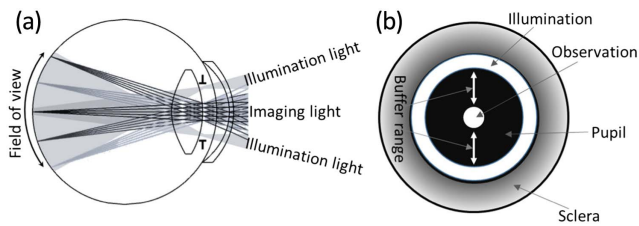
Fig. 1. Schematic diagram of the ring-shaped transpupillary illumination. (a) Side view of the illumination and imaging paths. (b) Front view of the illumination and observation paths. The ring-shaped illumination light is delivered through the periphery area of the pupil, and imaging light is collected for observation through the center of the pupil.

demonstrated a miniaturized indirect ophthalmoscopy-based smartphone fundus camera with a 61° external angle (92° eye angle) FOV [17,18]. This laboratory prototype device is mydriatic and requires pharmacological pupillary dilation. Here we refine and extend the miniaturized indirect ophthalmoscopy to construct a benchtop prototype fundus camera for wide-field non-mydriatic photography (Fig. 2).

Figure 2(a) illustrates the illumination strategy of the proposed miniaturized indirect ophthalmoscopy. Only one single spot at the pupil plane is utilized for indirect ophthalmoscopy illumination. For the system with single-spot illumination, only half of the pupil size is required to provide a similar buffer range as that in ring-shaped transpupillary illumination [Fig. 1(b)] to eliminate the effect of corneal reflection. With pharmacological dilation, the full pupil diameter is ~8 mm. In room light condition, a 4 mm pupil diameter can be readily achieved [19]. In dark light condition, the pupil diameter can be further enlarged without pharmacological dilation. Therefore, the miniaturized indirect ophthalmology illumination strategy holds potential for nonmydriatic fundus photography with a larger FOV compared to traditional ring-shaped transpupillary illumination.

Figure 2(b) illustrates the schematic diagram of the optical layout, and Fig. 2(c) shows a photograph of the benchtop prototype fundus camera based on the miniaturized indirect ophthalmoscopy. In addition to the eye lens of the testing subject, the optical imaging system consists of two optical lenses [L1 and L2 in Fig. 2(b)], one camera sensor (CS), and a light source (LS) [Fig. 2(b)]. The LS and lens L2 are in the same plane, with a 4 mm distance, to provide enough buffer range between illumination and observation paths to prevent the effect of corneal reflection on the fundus image. The LS/L2 plane is conjugated to the pupil plane P [Fig. 2(b)]. The intermediate

RI plane is conjugated to the retina and CS. Lens L1 is a 40 diopter (i.e., 25 mm focal length) ophthalmic lens to image the retina onto the plane RI [dashed vertical line, Fig. 2(b)] between the lens L1 and lens L2. Lens L2 is an 8 mm focal length F/2.5 micro video lens to relay the RI to the CS. The distance between L1 and L2 is 120 mm, and the distance to the subject pupil is 31.6 mm. Considering the 25 mm focal lens L1, the optical magnification from the subject pupil to the LS/L2 plane is 3.8×. Assuming the subject pupil diameter is 4 mm, the LS and L2 should be placed within a circular plane with a maximum diameter of 15.2 mm (4 × 3.8 mm). A CMOS camera (FL3-U3-120S3C-C, FLIR Integrated Imaging Solutions Inc., Richmond, Canada) was used for the benchtop prototype in Fig. 2(c). It has a frame size of 4000 × 3000 pixels, with a 1.55 μm × 1.55 μm pixel size and a 15 frames/second frame rate.

Instead of using a single visible LS as in our previous mydriatic prototype [17], the LS used in this nonmydriatic device consists of two illuminators: a near-infrared (NIR) [central wavelength, 850 nm] light-emitting diode (LED) (M850LP1, Thorlabs Inc., Newton, NJ) for preview mode imaging, i.e., for retinal positioning and focus adjustment; and a white LED (MWWHL4, Thorlabs Inc., Newton, NJ) for color retinal imaging. The NIR and white LEDs are coupled into one optical fiber [Fig. 2(c)], and the fiber end corresponds to the position of LS, which is conjugated with the illumination spot within the pupil plane P [LS′, Fig. 2(b)].

This human study was approved by the Institutional Review Board of the University of Illinois at Chicago and was in compliance with the ethical standards stated in the Declaration of Helsinki. Figure 3 shows representative images collected using the prototype fundus camera shown in Fig. 2(c). According to the ISO 15004-2:2007 standard [20], the weighted irradiance of the infrared and visible light were estimated as 0.06 mW/cm² and 0.22 mW/cm², respectively, at the retina. Therefore, the maximum exposure time for continuous illumination can be estimated as [20] $t_{max} = 10$ J/0.22 mW = 12.6 h.

The experiment was conducted in regular room light condition. First, the fundus camera was operated with NIR light illumination for retinal positioning and focusing adjustment. The NIR light guidance is required for nonmydriatic fundus photography because direct visible light illumination can induce pupil constriction within ~300 ms [21]. With NIR light guidance, we were able to capture at least three color fundus images before pupil constriction starts. We were aware of the slight difference between NIR and visible light foci. In order to optimize the quality of color fundus images, the NIR light was slightly defocused
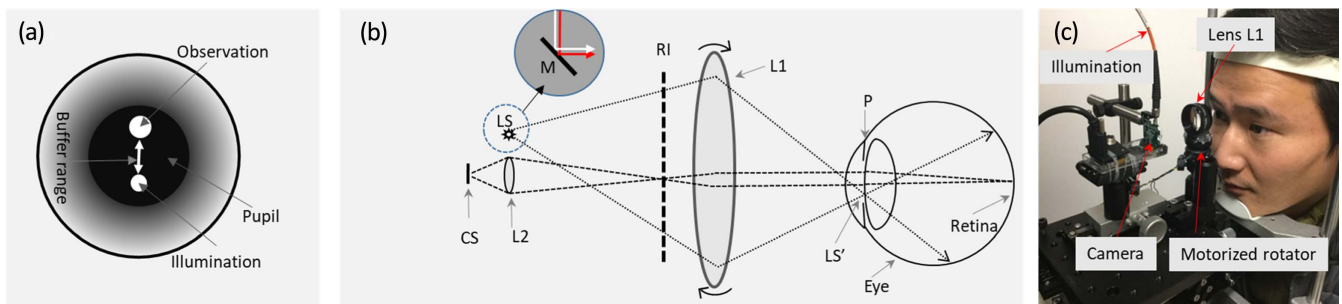

Fig. 2. (a) Schematic diagram of indirect ophthalmology illumination. (b) Optical layout of the miniaturized indirect ophthalmoscopy-based fundus camera. (c) Photograph of the bench-top prototype fundus camera.
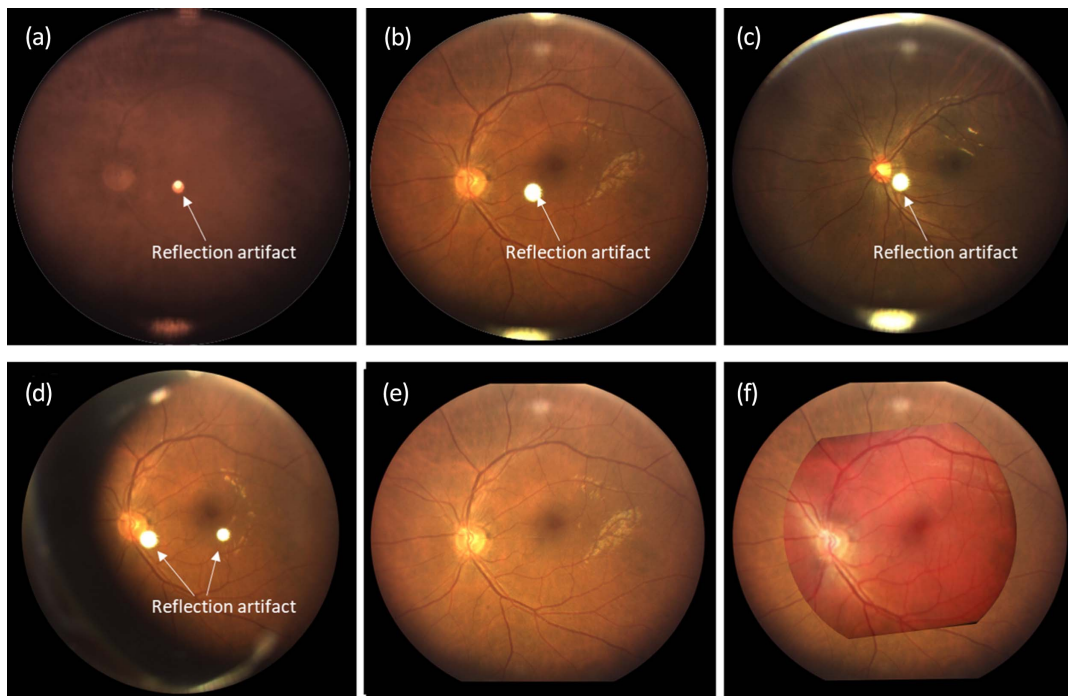
Fig. 3. Representative image captured using the prototype device in Fig. 2(c). (a) Near-infrared image captured during retinal location and focusing adjustment. (b) Color fundus image from a Caucasian volunteer subject. The reflection artifact is due to the light reflection of two surfaces of the lens L1. (c) Color fundus image from an Asian volunteer subject. (d) Another color fundus image from the same subject in Fig. 3(b). A motorized rotator [Fig. 2(c)] was used to rotate the optical axis of the lens L1 and, thus, to separate the two reflection spots which are overlapped in Fig. 2(b). (e) Artifact-free image, obtained from images in Figs. 3(b) and 3(d). (f) FOV comparison between the image Fig. 3(e) and a color fundus image captured using a commercial fundus camera (Volk Pictor Plus) from the same subject.

based on experimental calibration before the white light was triggered for color fundus imaging. Figure 3(a) shows a representative NIR image captured in preview mode. Figures 3(b) and 3(c) show color fundus images from Caucasian and Asian volunteers, respectively. The exposure time was set at 50 ms. According to the ISO 10940:2009 [9], a horizontal FOV was estimated as a 67° external angle (101° eye angle) with 23 μm resolution.

Reflection artifacts were observed in Figs. 3(a)–3(c). These reflection artifacts were due to the light reflection from the surfaces of lens L1. While the reflection artifact is not a problem for visual evaluation performed by clinicians, it can pose a challenge for automated image analysis and classification

in telemedicine applications. In principle, if two fundus images are captured, with the reflection artifacts shifted into different locations, digital compensation can be used to remove the reflection artifacts. In order to test the feasibility, a motorized rotator [Fig. 2(c)] was used to rotate the optical axis of the lens L1 to capture a second RI [Fig. 3(d)], following the image acquisition in Fig. 3(b). It took ~250 ms to collect the two images in Figs. 3(b) and 3(d), which is less than pupillary reaction time (~300 ms) for visible light illumination. The reflection artifacts due to two surfaces of the lens L1 were overlapped together in Fig. 3(b), while these two reflection spots were separated into two different locations by rotating the lens L1 in Fig. 3(d). The central parts of the images Figs. 3(b) and 3(d) were not affected
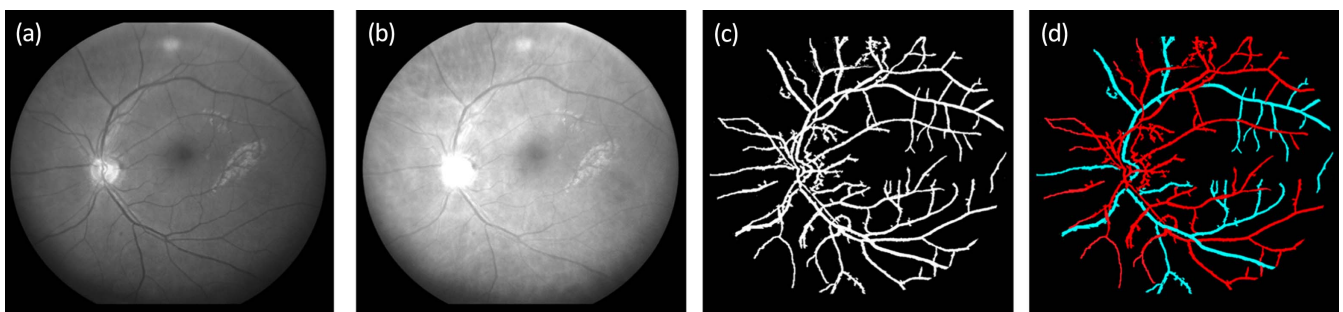

Fig. 4. Quantitative analysis of a representative color fundus image captured using the prototype fundus camera in Fig. 2(c). (a) Green channel of image Fig. 3(e). (b) Red channel of image Fig. 3(e). (c) Segmented blood vessel map based on Fig. 4(a). (d) Differential artery-vein map based on a density ratio analysis between (a) green and (b) red channels.

significantly. With the dual-image acquisition, digital image registration and glare elimination methods were used to remove reflection artifacts [Fig. 3(e)].

Figure 3(f) shows an overlapping illustration of the image Fig. 3(e) and another fundus image captured by a commercial fundus camera (Volk Pictor Plus, Volk Optical Inc., Mentor, OH) from the same subject. The Volk Pictor fundus camera provides a 45° external angle (68° eye angle) in a single-shot image. The comparative images further confirmed the FOV improvement of the miniaturized indirect ophthalmoscopy illumination-based fundus camera, compared to traditional fundus camera.

Quantitative analysis of fundus images is essential for objective and automated classification of eye diseases, which is particularly important for rural and underserved areas, or point-of-care environments. In order to verify the potential of using the miniaturized illumination-based wide-field fundus camera for quantitative image analysis, we used the image Fig. 3(e) to test automated blood vessel segmentation and artery-vein classification. As shown in Fig. 4, individual blood vessels can be readily identified [Fig. 4(c)], and arteries and veins can be differentiated based on optical density ratio analysis [Fig. 4(d)].

In summary, a miniaturized indirect ophthalmoscopy-based nonmydriatic wide-field fundus camera was demonstrated to achieve a 67° external angle (101° eye angle) FOV in single-shot images. A NIR light was used to guide nonmydriatic retinal imaging. True color fundus images revealed retinal structure and vasculature details [Fig. 3(f)]. For the proof-of-concept demonstration, the bench-top prototype in Fig. 3(c) was constructed using all off-the-shelf components. We anticipate that there is still a large room for further improvement of the FOV and image quality by professional optical design. Dual-image acquisition combined with digital data processing has been demonstrated to achieve reflection artifact-free color fundus imaging. As shown in Fig. 3(c), the system is simple; it can be readily packaged into a portable system and promises a next-generation, low-cost, and wide-field fundus camera for affordable telemedicine and point-of-care assessment of eye diseases.

REFERENCES

1. K. V. Chalam, V. S. Brar, and R. Keshavamurthy, Ophthalmic Res. **42**, 60 (2009).
2. J. A. Pugh, J. M. Jacobson, W. A. Van Heuven, J. A. Watters, M. R. Tuley, D. R. Lairson, R. J. Lorimor, A. S. Kapadia, and R. Velez, Diabetes Care **16**, 889 (1993).
3. W. M. Fierson and A. Capone, Jr., Pediatrics **135**, e238 (2015).
4. S. K. Wang, N. F. Callaway, M. B. Wallenstein, M. T. Henderson, T. Leng, and D. M. Moshfeghi, Can. J. Ophthalmol. **50**, 101 (2015).
5. M. T. Witmer and S. Kiss, Surv. Ophthalmol. **58**, 143 (2013).
6. A. Yuan, A. Kaines, A. Jain, S. Reddy, S. D. Schwartz, and D. Sarraf, Ophthalmic Surg. Lasers Imaging **41**, e1 (2010).
7. A. Nagiel, R. A. Lalane, S. R. Sadda, and S. D. Schwartz, Retina **36**, 660 (2016).
8. J. Aboshiha, A. M. Dubis, J. van der Spuy, K. M. Nishiguchi, E. W. Cheeseman, C. Ayuso, M. Ehrenberg, F. Simonelli, J. W. Bainbridge, and M. Michaelides, Ophthalmology **122**, 864 (2015).
9. ISO, "Ophthalmic instruments—fundus cameras—international standard," ISO 10940:2009 (2009).
10. K. Tran, T. A. Mendel, K. L. Holbrook, and P. A. Yates, Invest. Ophthalmol. Visual Sci. **53**, 7600 (2012).
11. E. DeHoog and J. Schwiegerling, Appl. Opt. **47**, 6769 (2008).
12. D. A. Salz and A. J. Witkin, Middle East Afr. J. Ophthalmol. **22**, 145 (2015).
13. A. Russo, F. Morescalchi, C. Costagliola, L. Delcassi, and F. Semeraro, J. Ophthalmol. **2015**, 823139 (2015).
14. R. N. Maamari, J. D. Keenan, D. A. Fletcher, and T. P. Margolis, Br. J. Ophthalmol. **98**, 438 (2014).
15. A. Samaniego, V. Boominathan, A. Sabharwal, and A. Veeraraghavan, in *Frontiers in Optics*, OSA Technical Digest (online) (Optical Society of America, 2014), paper FW3F.1.
16. D. Toslak, D. Thapa, Y. Chen, M. K. Erol, R. V. Paul Chan, and X. Yao, Opt. Lett. **41**, 2688 (2016).
17. D. Toslak, A. Ayata, C. Liu, M. K. Erol, and X. Yao, Retina **38**, 438 (2018).
18. D. Toslak and X. C. Yao, "Miniaturized indirect ophthalmoscopy for wide-field fundus photography," U.S. patent US 62/546,830 (August 17, 2017).
19. E. Alexandridis, *Pupil Size* (Springer, 1985), p. 11.
20. ISO, "Ophthalmic instruments—fundamental requirements and test methods—part 2: light hazard protection," ISO 15004-2:2007 (2007).
21. O. Bergamin and R. H. Kardon, Invest. Ophthalmol. Visual Sci. **44**, 1546 (2003).